

# DESIGN AND FABRICATION OF A CENTRIFUGALLY DRIVEN MICROFLUIDIC DISK FOR FULLY INTEGRATED METABOLIC ASSAYS ON WHOLE BLOOD

J. Steigert<sup>1</sup>, T. Brenner<sup>1</sup>, M. Grumann<sup>1</sup>, L. Riegger<sup>1</sup>, R. Zengerle<sup>1,2</sup>, and J. Duccr e<sup>2</sup>

<sup>1</sup>University of Freiburg – IMTEK, Laboratory for MEMS Applications,  
Georges-Koehler-Allee 106, D-79110 Freiburg, Germany

<sup>2</sup>HSG-IMIT, Wilhelm-Schickard-Strasse 10, D-78052 Villingen-Schwenningen, Germany  
e-mail: steigert@imtek.de

## ABSTRACT

For the first time, we present a novel and fully integrated centrifugal microfluidic “lab-on-a-disk” for rapid metabolic assays in human whole blood. All essential steps comprising blood sampling, metering, plasma extraction and the final optical detection are conducted within  $t = 150$  s in passive structures integrated on one disposable disk. Our technology features a novel plasma extraction structure ( $V = 500$  nL,  $CV < 5\%$ ) without using any hydrophobic microfluidics where the purified plasma ( $c_{RBC} < 0.11\%$ ) is centrifugally separated and subsequently extracted through a capillary primed extraction channel into the detection chamber. While this capillary extraction requires precisely defined, narrow microstructures, the reactive mixing and detection is most efficient within larger cavities. The corresponding manufacturing technique of these macro- and micro structures in the range of  $30 \mu\text{m}$  to  $1000 \mu\text{m}$  is also presented for the first time: A novel, cost-efficient hybrid prototyping technique of a multiscale epoxy master for subsequent hot embossing of polymer disks.

## 1. INTRODUCTION

The transfer of routines in clinical diagnostics to compact point-of-care devices is subject of various academic [1]-[4] and commercial efforts [5][6]. An important objective in medical diagnostic systems is the integration of the full process chain from the preparation of a patient's whole blood to an analytical result. To meet the requirements of clinical diagnostics, so called „lab-on-a-chip“ or „ $\mu$ TAS“ (micro total analysis systems) which feature a full process integration, reduced consumption of sample and reagents as well as short times-to-result and ease of handling are the most prominent candidates.

Various lab-on-a-chip systems have proven to carry out these processing steps, among them centrifugal “lab-on-a-disk” [7] devices which exploit inertial and capillary forces for sample preparation and flow control [8]-[10]. Their high potential to run complete assay protocols, starting from raw whole blood, is reflected by the intrinsic pumping and separation mechanisms based on the centrifugal field. Several microfluidic approaches for a batch separation

[7][10][11] of blood and metering of a defined volume of purified plasma [9][12][13] based on hydrophobic microfluidics have been presented so far. We focus on the implementation of a disk-based sample preparation structure which combines the blood sedimentation and plasma metering in one single structure. The functionality is demonstrated by a colorimetric absorption assay to determine the alcohol concentration in untreated human whole blood.

## 2. SETUP

We use a hot embossed polymer substrate (COC) with the size of a common compact disk (CD). The substrate features fluidic and optical elements to perform colorimetric assays. The fluidic elements provide ports for sample and reagent uptake as well as a sample preparation structure with integrated blood sedimentation and plasma metering which is connected to a combined mixing and detection chamber (Fig. 1). The liquid transport is controlled by the centrifugal force  $F_v$ , which is generated by spinning of the passive disk.

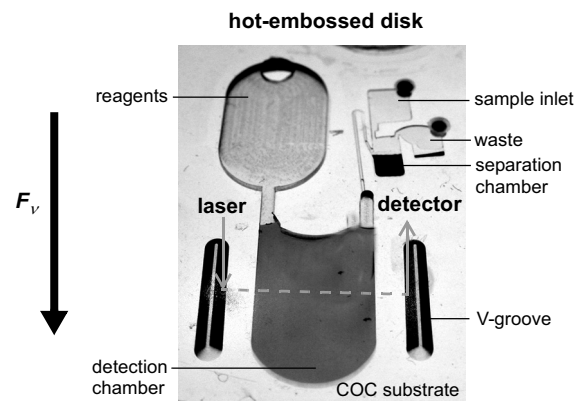


**Figure 1.** The hot embossed disk features all required optical and microfluidic structures to perform an enzymatic absorption assay to determine the alcohol concentration in human whole blood.

## 3. PLASMA EXTRACTION STRUCTURE

The basic structure in Fig. 2 consists of a separation chamber which is connected to one inlet for the blood sample and two

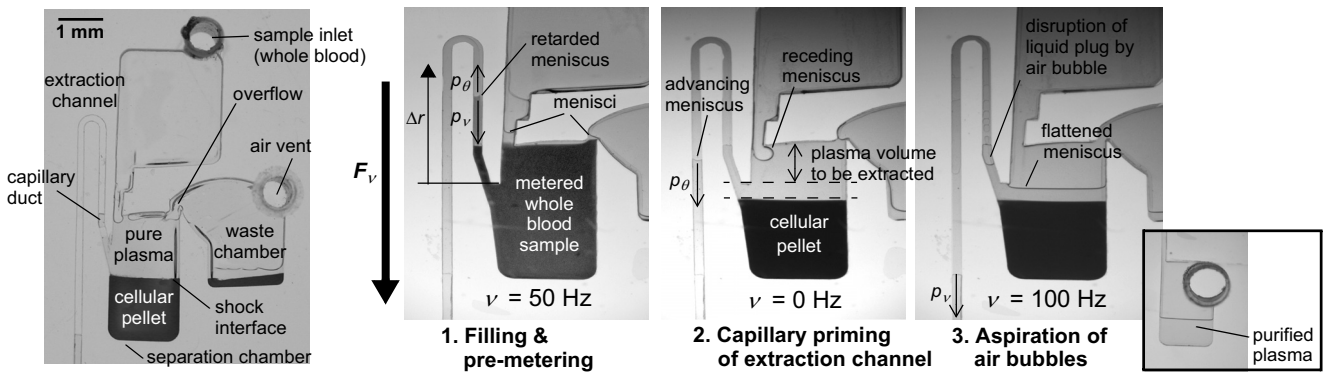


**Figure 2.** Section view of the plasma extraction structure. (1) After injection through the inlet, a droplet of raw blood is metered by the overflow channel. Three menisci can be identified in the inlet and both outlets. (2) The cells settle towards the bottom of the reservoir as the shock interface separating pure plasma and cellular blood proceeds. Once the shock interface is below the inlet of the plasma extraction channel, the disk is stopped and the extraction channel is filled by the capillary pressure  $p_\theta$ . (3) A net radial length  $\Delta r < 0$  induces a centrifugal pressure  $p_v$  to pump the plasma through the extraction channel. The extraction process ceases at the point when air is sucked into the plasma extraction channel. This point is reproducibly defined ( $CV < 1\%$ ) by the centrifugally supported flattening of the meniscus towards high spinning frequencies. The extracted plasma is collected in a reservoir attached to the extraction channel for further use.

outlets. One outlet is an overflow to initially meter the raw blood sample, the other outlet represents a plasma extraction channel which bends at a radial position located further inward than the maximum liquid level in the inlet structure.

The hydrodynamic behavior of the extraction channel depends on the radial spacing  $\Delta r$  between its downstream meniscus with respect to the liquid level in the inlet structure. As long as the meniscus in the plasma extraction channel stays radially inward with respect to the liquid level ( $\Delta r > 0$ ), liquid is retained at all frequencies within the sedimentation and metering compartment according to the principle of interconnected tubes. The extraction channel is primed by lowering the frequency  $\nu$  below a threshold  $\nu_{crit}$  where the capillary pressure surpasses the (initially) counteracting centrifugally induced hydrostatic pressure. As soon as a net radial length  $\Delta r < 0$  emerges in the capillary priming, the liquid can be pumped centrifugally to downstream structures until the continuous liquid column is disrupted.

The frequency protocol for the metering, sedimentation and plasma extraction with the structure (Fig. 2) is displayed in Fig. 3. By spinning for 2 s with a frequency  $\nu = 50$  Hz, the

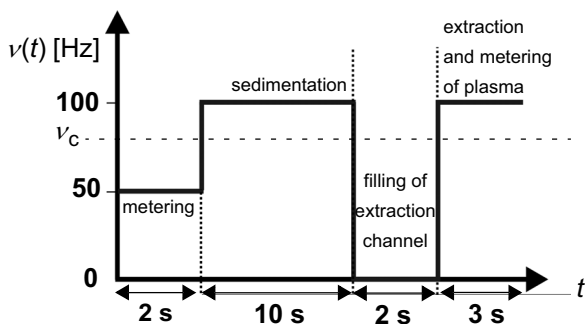


**Figure 3.** Frequency protocol of the sample preparation step with integrated blood sedimentation and extraction of highly purified plasma.

separation chamber is filled and a volume is defined via the overflow structure. Raising  $\nu$  to 100 Hz for 10 s leads to a rapid sedimentation of the whole blood. Now the spinning frequency is reduced, *i.e.*  $\nu < \nu_{crit}$ , for  $t = 2$  s to prime the plasma extraction channel. Once the meniscus has reached a position  $\Delta r < 0$ , the frequency is increased again to extract the plasma. The extraction ceases when gas is drawn into the extraction channel. The point of disruption is geometrically defined by the position of the edge as well as the hydrodynamic control of the break-off process to enable the precise metering of the extracted amount of plasma. We achieve a high volumetric precision of the extracted plasma in the detection chamber ( $V = 500$  nl) with a  $CV$  better than 1%

The speed of sedimentation is proportional to  $1/\nu^2$  (Fig. 4) whereas the separated volume only depends on the volume capacity of the separation chamber. A residual cell concentration in the plasma  $c_{RBC} < 0.11\%$  is determined by optical comparison to calibrated cell suspensions.

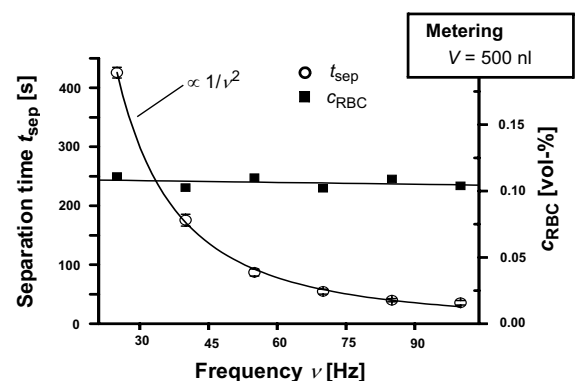


**Figure 4.** The measured separation time  $t_{sep}$  of the metered 500-nl blood volume ( $CV < 1\%$ ) decreases with the inverse square of the spinning frequency  $\nu$ . The quality of the extracted plasma represented by the residual red blood cell concentration  $c_{RBC}$  remains below 0.11% for all  $\nu$ .

#### 4. INTEGRATED ABSORPTION ASSAY

An integrated absorption assay is conducted by a fully automated frequency protocol to eliminate all error-prone handling steps. To carry out the absorption assay, the extracted plasma in the detection chamber is efficiently mixed with enzymatic reagents [14] by using “shake-mode” mixing which means a frequent reversal of the sense of rotation [15]. Finally, the absorbance correlating to the alcohol concentration is monitored in real-time during constant spinning [16] with our previously introduced optical total internal reflection (TIR) setup [17]. By benchmarking with calibrated samples [18], our measurements (Fig. 5) display a  $CV$  of 5.3%, a lower limit of detection  $c_{\min} = 0.05\%$ , an excellent resolution ( $\Delta c = 0.06\%$ ), and a high linearity between the alcohol concentration and the optical absorption signal ( $R^2 = 0.996$ ). Additionally, the real time monitoring under rotation allows to drastically reduce the time-to-result with respect to standard kits. This performance is comparable to common breath analyzers while avoiding the error prone correlation between the alcohol concentration in breath and whole blood.

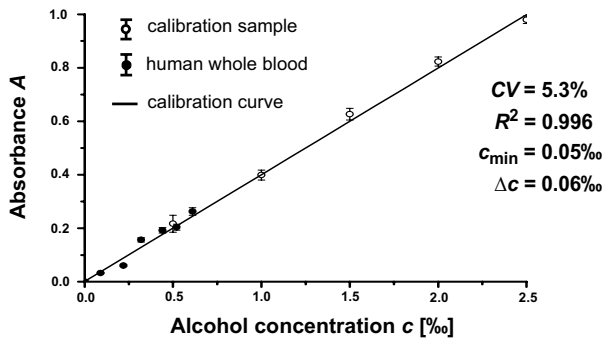


**Figure 5.** Calibration curve of the alcohol assay. After sedimentation and mixing is completed, the increase of the absorbance  $A$  is recorded. Our measurements well reproduce the concentrations of calibrated ethanol solutions as well as reference measurements on human whole blood with a  $CV$  of 5.3%, a lower limit of detection  $c_{\min} = 0.05\%$ , a resolution of  $\Delta c = 0.06\%$ , and a linearity of  $R^2 = 0.996$ .

#### 5. MASTER FABRICATION

We developed a multistep hot embossing process to fabricate the multiscale structures (Fig. 6). First, micro structures were patterned on a Pyrex wafer by backside SU-8 lithography, cast in PDMS and subsequently cast in a mechanically and thermally stable epoxy resin (“epoxy-master 1”) [19]. The “epoxy master 1”, exhibiting the micron-scale structures ( $30\ \mu\text{m} - 100\ \mu\text{m}$ ), is transferred by hot embossing into an intermediate COC substrate. Next, the macro structures ( $1000\ \mu\text{m}$ ) are added by micromilling. In the final step, this intermediate is cast into the “epoxy master 2”.

This novel hybrid tooling technology allows rapid (less than two days) and cost-efficient fabrication of multiscale hot embossing masters (Fig. 7). The maximum depth of masters

merely based on SU-8 lithography is limited to about  $300\ \mu\text{m}$  [19]. CNC micromachining of the intermediate COC master allows to incorporate deeper structures (up to several millimeters) for larger reaction and detection cavities which are also no longer restricted to a rectangular shape. The mechanically and thermally stable master could be used both in hot embossing and injection molding.

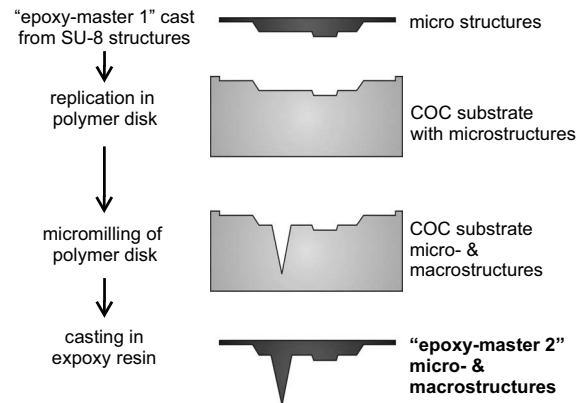


**Figure 6.** Fabrication process for epoxy masters. A polymer disk is hot embossed from an intermediate “epoxy master 1” which features only micro structures and post-processed via micromilling to enable deeper macro structures. A mechanically and thermally stable hot embossing “epoxy master 2” is fabricated in an additional casting step. The structures of the “epoxy master 2” are versatile in depth and shape.

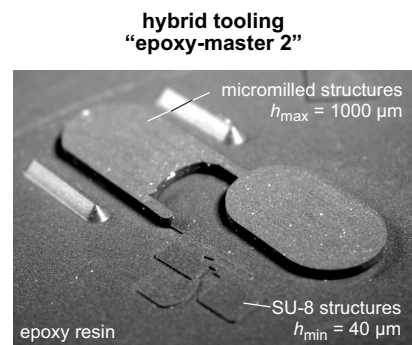


**Figure 7.** Photograph of the epoxy master which features structures in variation of shape and size, i.e. channel depths from  $40\ \mu\text{m}$  to  $1000\ \mu\text{m}$ .

#### 6. CONCLUSION

We introduced a novel, centrifugal sample preparation scheme for whole blood displaying an integrated metering and plasma extraction. Its performance was successfully demonstrated in a fully process integrated enzymatic absorbance assay on alcohol. The assay is conducted by an automated frequency protocol to eliminate error-prone handling steps. The basic operation functions of our integrated sedimentation and metering structure, like stopping, metering and / or valving a flow are achieved by implementing an extraction channel without hydrophobic microfluidics. In respect to common structures which are mostly based on capillary burst valves our

setup displays a strong simplification in the fabrication process.

In addition, the here presented multi-step fabrication of the epoxy-based hot embossing master allows to replicate microfluidic chips with variable range structure depths in a very rapid and cost-efficient fashion.

### ACKNOWLEDGEMENT

The authors are grateful to the partial support by the Ministry of Science, Research and the Arts of the German federal state of Baden-Wuerttemberg (contract 24-720.431-1-7/2) and the good cooperation with Jobst-Technologies.

### REFERENCES

- [1] Sia, S.; Linder, V.; Parviz, B.; Siegel, A.; Whitesides, G. *Angew. Chem. Int.* **2004**, 43, 498-502.
- [2] Vilkner, T.; Janasek, D.; Manz, A. *Anal. Chem.* **2004**, 76, 3373-3386.
- [3] Reyes, D.; Iossifidis, D.; Auroux, P.; Manz, A. *Anal. Chem.*, **2002**, 74, 2623-2636.
- [4] Auroux, P.; Reyes, D.; Iossifidis, D.; Manz, A. *Anal. Chem.*, **2002**, 74, 2637-2652.
- [5] Ducreé, J.; Zengerle, R. *FlowMap - Microfluidics roadmap for the life sciences*, **2004**, Books on Demand GmbH: Norderstedt, Germany, ISBN 3-8334-0744-1, www.microfluidics-roadmap.com.
- [6] Schembri, C.; Burd, T.; Kopf-Sill, A.; Shea, L.; and Braynin, B., *Journal of Automatic Chemistry*, **1995**, 17 (3), 99-104.
- [7] Madou, M. J.; Kellogg, G. J. *Proc of SPIE*, 1998, 3259, 80-93.
- [8] Puckett, L.; Dikici, E.; Lai, S.; and Madou, M. *Anal. Chem.*, **2004**, 76, 7263-7268.
- [9] Ekstrand, G.; Holmquist, C.; Örforn, A. E.; Hellmann, B.; Larsson A.; and Andersson, P. *Proc. of  $\mu$ TAS*, 2000, 311-314.
- [10] Thorsén, G.; Ekstrand, G.; Selditz, U.; Wallenborg, S. R., and Andersson, P. *Proc. of  $\mu$ TAS*, 2003, 457-460.
- [11] Brenner, T.; Haerberle, S.; Zengerle, R.; Ducreé, J. *Proc. of  $\mu$ TAS*, 2004; 566-569.
- [12] Zeng, J.; Banerjee, D.; Deshpande, M.; Gilbert, J.; Duffy, C. D.; Kellogg, D. J. *Proc. of  $\mu$ TAS*, 2000, 579-582.
- [13] Mc Neely, M. R.; Spute, M. K.; Tusneem, N. A.; Oliphjat, A. R. *Proc. of SPIE*, 1999, 3877, 210-220.
- [14] ALK 121, Diaglobal GmbH, Germany, www.diaglobal.de
- [15] Grumann, M.; Geipel, A.; Riegger, L.; Zengerle, R.; Ducreé, J. *LOC*, **2005**, 5, 560-565.
- [16] Steigert, J.; Riegger, L.; Grumann, M.; Brenner, T.; Harter, J.; Zengerle, R.; Ducreé, J. *Proc. of  $\mu$ TAS*, 2005, 1, 1-3.
- [17] Grumann, M.; Moser, I.; Steigert, J.; Riegger, L.; Geipel, A.; Kohn, C.; Urban, G.; Zengerle, R.; Ducreé, J. *Proc. of MEMS*, 2005, 08-112.
- [18] ALK QS, Diaglobal GmbH, Germany, www.diaglobal.de
- [19] Brenner, T.; Gottschlich, N.; Knebel, G.; Mueller, C.; Reinecke, H.; Zengerle, R.; Ducreé, J. *Proc. of  $\mu$ TAS*, 2005, 1, 193-195.